

# Tenors not sopranos: Bio-mechanical constraints on calling song frequencies in the Mediterranean field-cricket

1 Thorin Jonsson<sup>1\*</sup>, Fernando Montealegre-Z.<sup>2\*</sup>, Carl D. Soulsbury<sup>2</sup>, Daniel Robert<sup>3</sup>

2 <sup>1</sup> Institute of Biology, Karl-Franzens-University Graz, Universitätsplatz 2, 8010 Graz, Austria

3 <sup>2</sup> School of Life Sciences, University of Lincoln, Joseph Banks Laboratories, Lincoln, LN6 7DL, UK

4 <sup>3</sup> School of Biological Sciences, University of Bristol, Tyndall Avenue, Bristol, BS8 1TQ, UK

## 5 \*Correspondence:

6 Thorin Jonsson, thorin.jonsson@uni-graz.at

7 Fernando Montealegre-Z, fmontealegrez@lincoln.ac.uk

8 **Keywords:** coupled resonators, bioacoustics, insect communication, biomechanics, Ensifera

## 9 Abstract

10 Male crickets and their close relatives bush-cricket (Gryllidae and Tettigoniidae, respectively;  
11 Orthoptera, Ensifera) attract distant females by producing loud calling songs. In both families, sound  
12 is produced by stridulation, the rubbing together of their forewings, whereby the plectrum of one wing  
13 is rapidly passed over a serrated file on the opposite wing. The resulting oscillations are amplified by  
14 resonating wing regions. A striking difference between Gryllids and Tettigonids lies in wing  
15 morphology and composition of song frequency: Crickets produce mostly low-frequency (2-8 kHz),  
16 pure tone signals with highly bilaterally symmetric wings, while bush-cricket use asymmetric wings  
17 for high-frequency (10-150 kHz) calls. The evolutionary reasons for this acoustic divergence are  
18 unknown. Here, we study the wings of actively stridulating male field-cricket (*Gryllus bimaculatus*)  
19 and present vibro-acoustic data suggesting a biophysical restriction to low-frequency song. Using laser  
20 Doppler vibrometry and brain-injections of the neuroactivator eserine to elicit singing, we recorded the  
21 topography of wing vibrations during active sound production. In freely vibrating wings, each wing  
22 region resonated differently. When wings coupled during stridulation, these differences vanished and  
23 all wing regions resonated at an identical frequency, that of the narrow-band song (~5 kHz). However,  
24 imperfections in wing-coupling caused phase shifts between both resonators, introducing destructive  
25 interference with increasing phase differences. The effect of destructive interference (amplitude  
26 reduction) was observed to be minimal at the typical low frequency calls of crickets, and by maintaining  
27 the vibration phase difference below 80°. We show that, with the imperfect coupling observed, cricket  
28 song production with two symmetric resonators becomes acoustically inefficient above ~8 kHz. This  
29 evidence reveals a bio-mechanical constraint on the production of high-frequency song whilst using  
30 two coupled resonators and provides an explanation as to why crickets, unlike bush-cricket, have not  
31 evolved to exploit ultrasonic calling songs.

32 **1 Introduction**

33 Male crickets (Ensifera, Gryllidae) produce loud musical songs to attract conspecific females  
 34 by rubbing their raised forewings together, a process known as stridulation. During stridulation,  
 35 the plectrum – a sharp sclerotized region at the anal edge of the left wing (LW) – engages with the  
 36 file, a row of teeth on a modified, serrated vein on the underside of the right wing (RW) in a  
 37 clockwork-like manner (Elliott and Koch, 1985; Prestwich et al., 2000). In Gryllidae, the RW usually  
 38 sits on top of the LW, and during stridulation, both wings open and close in a rhythmic cycle,  
 39 with sound being generated during the closing phase only (Koch et al., 1988; Bennet-Clark, 1999).  
 40 The dorsal field of each bilaterally symmetric wing displays a number of clearly delineated wing  
 41 cells involved in sound radiation. These are the harp, mirror, chord, and the hardened, non-  
 42 membranous anal surface (Montealegre-Z et al., 2011) (Fig. 1).

43 The male is under strong sexual selection to sing at a high amplitude in order to effectively attract  
 44 and provide phonotactic information for distant females (Forrest and Green, 1991; Römer, 1998). In  
 45 most cricket species, acoustic energy is concentrated within a narrow-band, pure-tone signal  
 46 centred on a single low-frequency carrier (~5 kHz in the case of the field-cricket *Gryllus*  
 47 *bimaculatus* De Geer) which is amplified and radiated by wing regions functioning as natural  
 48 resonators (Bennet-Clark, 1999, 2003). A loud, pure-tone calling song extends the signal range,  
 49 aiding the females in determining the direction of the sound source through the enhancement of  
 50 binaural hearing (Kostarakos et al., 2008; Michelsen and Larsen, 2008) and makes it possible  
 51 to obtain a large signal-to-noise ratio for transmission across the environment (Michelsen, 1998;  
 52 Warren et al., 2006; Wiley, 2006). For optimal power transfer from sound source to the surrounding  
 53 medium, a resonator like the cricket wing should have a radius of at least  $1/6$  of the sound  
 54 wavelength  $\lambda$  ( $\lambda = \sim 7$  cm at 5 kHz; assuming a monopole radiator; the radius increases to  $1/4-1/3\lambda$   
 55 for dipoles) (Fletcher, 1992; Bennet-Clark, 1998). Small, sound-producing insects like crickets  
 56 with wings about 0.5-1 cm in size are therefore under strong selection to optimize power output  
 57 in order to maximize signal range. Crickets approach this optimization problem by using  
 58 both symmetric forewings together as sound radiators during stridulation to increase the sound  
 59 radiating surface for low-frequency songs (Bennet-Clark, 1999, 2003; Montealegre-Z et al., 2011). In  
 60 contrast, their close relatives bush-crickets (Tettigoniidae) have evolved high-frequency singing using  
 61 asymmetric wings as a derived trait where the overlying LW bears the file and is usually  
 62 mechanically dampened, while the plectrum-bearing RW is highly adapted for efficient sound  
 63 radiation (e.g. Montealegre-Z and Postles, 2010; Sarria-S et al., 2016; Song et al., 2020). The  
 64 drivers for the evolution of this asymmetry are unknown but it has been hypothesised to be linked to  
 ultrasonic sound production and signal purity (Montealegre-Z, 2005; Gu et al., 2012)

65  
 66 Signal transmission is facilitated by resonance– an inexpensive way of enhancing sound output while  
 67 conserving metabolic energy – whereby the call's carrier frequency ( $f_c$ ) is determined by the  
 68 resonance frequency  $f_0$  of the wings, which implies that both wings in a symmetric system should  
 69 resonate at similar  $f_0$ . Reliance on two coupled resonant structures requires that crickets have to  
 70 achieve and maintain a high degree of phase locking between the two wings in order to add vibrations  
 71 constructively (Prestwich et al., 2000). Only when the two resonators are vibrating at similar  $f_0$  with  
 72 minimal phase differences ( $\phi$ ) is constructive wave superposition providing the desired effect of  
 73 increasing the amplitude of radiated sound energy. When optimal ( $\phi=0$ ), this constructive  
 74 interference results in a doubling of the amplitude of the combined output (Rossing, 1990). How can  
 this behaviour, defined here as in-phase, take place?

75  
 76 The in-phase resonance between wings is facilitated by an escapement mechanism that allows  
 both wings to vibrate together and radiate sound efficiently (Koch et al., 1988). However, prior  
 mechanical

77 analyses of cricket stridulation showed that the mechanism of sound production is asymmetrical  
 78 (Bennet-Clark, 2003; Montealegre-Z, 2005; Montealegre-Z et al., 2011): While the RW receives its  
 79 energy input along the file's ca. 200 teeth distributed over a distance of some 4 mm, the underlying  
 80 LW receives energy only through the small region of the plectrum ( $0.1 \text{ mm}^2$ , Fig. 1B). Figure 1B shows  
 81 that as the plectrum is dragged on the file from left to right, it generates mechanical impacts at different  
 82 locations along the file. The input of mechanical energy therefore varies in time and location,  
 83 potentially resulting in a complicated dispersion of substrate-borne waves across the surface area of  
 84 the RW (Fig. 1B left). On the other hand, the LW has only one input, the plectrum, and vibrations will  
 85 travel constantly to the various LW regions from that input (Fig. 1B right). Therefore, the LW should  
 86 vibrate with constant phase, independently of the plectrum's position on the RW. In contrast, the RW  
 87 should be more vulnerable to phase changes as the moving plectrum delivers energy impulses along  
 88 the file. If these assumptions hold true, the constant phase generator (LW) and the variable phase  
 89 generator (RW) are expected to interact and generate beats in their summed acoustic output, in  
 90 particular at locations where LW and RW vibrations cancel each other out (Sismondo, 1993). Yet, the  
 91 natural song of the male does not exhibit such beats; instead, song pulses have sustained and regular  
 92 amplitude and phase profiles.

93 In addition, it is also implied that the wings' resonances are perfectly in tune with the input stimulus,  
 94 each wings'  $f_0$  is equal to the song carrier frequency  $f_c$ . However, previous studies revealed that the left  
 95 and right wings exhibit different  $f_0$ , above and below the output  $f_c$  ( $<5 \text{ kHz}>$ ) (Nocke, 1971; Bennet-  
 96 Clark, 2003; Montealegre-Z et al., 2011). Non-contact laser Doppler vibrometry (LDV) measurements  
 97 showed that the left and right wings of field-crickets are mechanically different, with resonant  
 98 frequencies differing by as much as 2 kHz ( $f_{0 \text{ left}} < f_{0 \text{ right}}$ ; Montealegre-Z et al., 2011). It remains unclear  
 99 how the seemingly imperfect and differently tuned resonators can generate the high quality pure-tones  
 100 observed in crickets.

101 Using LDV, focal microinjection of the neuropharmacological neuroactivator eserine, and specialized  
 102 acoustic equipment, we measured wing vibrations in actively stridulating Mediterranean field-crickets  
 103 (*Gryllus bimaculatus*). From physical acoustics, we hypothesise that efficient, high gain, pure-tone  
 104 radiation results from the in-phase oscillation of both wings when coupled during the stridulation  
 105 process. We furthermore formulate and test a second hypothesis: different wing regions vibrate in  
 106 phase, despite differential tuning and inputs, and thereby generate the coherent acoustic radiation  
 107 typical of field-cricket songs.

108 As a consequence, any imperfections in the coupling of the wings that lead to temporal and phase shifts  
 109 between the resonators should result in sub-optimal amplitude of the output signal and ultimately  
 110 impose constraints on signal frequency.

111

## 112 2 Material & Methods

### 113 2.1 Animals

114 Adult male crickets (*G. bimaculatus*) obtained from a breeding colony maintained at the University of  
 115 Bristol were used. Animals were kept at room temperature (20-22 °C) under a 12h:12h light:dark cycle  
 116 and were fed with oats, dry dog food and water *ad libitum*. Adult males were randomly taken from the  
 117 colony, their wings inspected for damage and kept individually in cages prior to the experiments. After  
 118 isolation, 18 males that sang for prolonged periods of time were chosen for the experiments, as these

119 animals usually responded better to pharmacological stimulation. All males recorded were singing with  
120 the usual wing overlap (RW over LW).

## 121 **2.2 Neuropharmacological stimulation**

122 To elicit persistent stridulation in tethered crickets, we followed methods established and described in  
123 detail in earlier studies (Hedwig and Becher, 1998; Wenzel et al., 1998; Wenzel and Hedwig, 1999;  
124 Montealegre-Z et al., 2011). In short, we used borosilicate glass microcapillaries (1B120F-3; ID=0.68  
125 mm; World Precision Instruments, Inc., Sarasota, FL, USA) pulled with a Sutter microelectrode  
126 puller (Sutter Instrument Company, Novato, California, USA) to produce ca. 10  $\mu\text{m}$  wide tips. These  
127 microcapillaries were then filled with eserine/ringer solution ( $10^{-2}$  mol  $\text{l}^{-1}$ ; Sigma-Aldrich Company  
128 Ltd., Dorset, UK) and connected to a picospritzer (Picospritzer II, Parker Hannifin, Pneutronics  
129 Division (formerly General Valve), NJ, USA). Small quantities of eserine (an acetylcholinesterase  
130 inhibitor) were injected into a brain neuropil, located in between the pedunculus and the  $\alpha$ -lobe of the  
131 mushroom bodies. Successful procedures elicited sustained stridulation in the typical calling song  
132 pattern (see Supplementary Video 1). Crickets were removed from the study if we recorded no  
133 singing activity within 1 hour after the first injection.

134 Crickets exhibit frequency modulation (FM) in their calls, and the envelope of this modulation has  
135 been shown to be a fingerprint of each individual (Montealegre-Z et al., 2011). The quality of the  
136 pharmacologically elicited calls was examined by correlating their FM pattern with that of the natural  
137 calls obtained by zero-crossing analysis. Calls were judged of sufficient quality when the correlation  
138 was higher than 0.85 (see Montealegre-Z et al., 2011, for more experimental details).

## 139 **2.3 Recordings of wing vibrations in stridulating animals (wings engaged)**

140 Vibrations from the tegminal surface were successfully quantified from 11 of the 14 stridulating  
141 animals using two coupled laser Doppler vibrometers (Polytec PSV-300-F, and a PSV-400; Polytec  
142 GmbH, Waldbronn, Germany) and corresponding scanning heads (OFV-056) fitted with close-up  
143 attachments. The velocity output of the PSV-300-F served as an input channel for the PSV-400  
144 vibrometer, thus allowing for synchronization of the recordings. Sound signals were recorded using a  
145 1/8" condenser microphone Brüel & Kjær Type 4138, connected to a Brüel & Kjær 2633  
146 preamplifier (Brüel & Kjær, Nærum, Denmark), which was in turn connected to the PSV-400  
147 acquisition system. Measurements were performed in single-shot mode (one recording per chosen  
148 spot on the wing, no averaging) mode in the temporal domain (1024 samples at 512 kHz sampling  
149 rate, leading to recordings with 2 ms duration and a temporal resolution of  $\sim 1.95$   $\mu\text{s}$ ). Acoustic and  
150 vibrational measurements were recorded with Polytec Scanning Vibrometer software (PSVSoft,  
151 Version 8, Polytec GmbH, Waldbronn, Germany). The microphone was positioned posterior to the  
152 specimen, 3-4 cm away from the wings as to not interfere with the laser beams. Simultaneously, wing  
153 vibrations were recorded with the laser beams focused on the anal regions, harps, chords and mirrors  
154 (Fig. 1 and see Supplementary Video 1 showing a singing male after pharmacological stimulation).  
155 Through the video feed of the two LDVs, we were able to visually place the laser points with some  
156 acuity within the regions in question, ensuring that the recordings from left and right wing came from  
157 equivalent locations. Results for the chord regions are shown in the supplementary material section  
158 but are not included in the main results as we were able to obtain chord recordings in only 7 out of  
159 the 11 animals used (the left chord regions are usually covered by the RW during stridulation and  
160 thus not easily accessible). The laser spot position and signal strength (the amount of laser light  
161 reflected from the target) was monitored and controlled via the live video feeds to the controlling  
162 computers of both laser systems. Using earlier LDV systems, signal strength often had to be  
163 increased by applying minute reflecting beads or powder to the wing surfaces. This was not the case  
here as the focussed laser light ( $\lambda \sim 630$  nm) waswell

164 reflected by the wing cuticle, which allowed us to perform contactless vibration measurements without  
165 further manipulation of the wings.

166 The microphone signal was used as a measurement trigger, so only wing vibrations involved in sound  
167 production were recorded. Data acquisition was programmed to last for 2 ms during the  
168 maximum amplitude event of a song pulse. This duration was chosen to minimise the movement  
169 of the wings during recording (~ 8-10 teeth) while still gathering sufficient data for analysis (see also  
170 Montealegre-Z et al., 2011).

#### 171 **2.4 Individual resonances of unengaged fixed wings (free vibration)**

172 After the previous experiment, each of the wings of each live specimen (n=14) were extended and  
173 separated from each other by fixing the axillary sclerites with a bee's wax (Fisher Scientific UK,  
174 Limited, Leicestershire; product code W/0200/50), and Colophony (Sigma-Aldrich Co. St. Louis, MO,  
175 USA; Product No. 60895-250G) mixture (1:1). The wings were extended to not be in contact with the  
176 pronotal lateral and posterior edges. A loudspeaker (ESS AMT-1; ESS Laboratory Inc., Sacramento,  
177 CA, USA) was used to broadcast periodic chirps in the range 1-20 kHz, with a flat (55 dB SPL  $\pm$  1.5  
178 dB) spectrum. The microphone was placed dorsally in the middle of both extended wings (Fig. 4). The  
179 laser system was set to record in the scan mode. A complete scan of the extended wings in response to  
180 the periodic chirps was performed with the PSV-400 LDV, using 250-300 scanning points per wing  
181 with 10 measurements averaged per point. FFT with a rectangular window and a sampling rate of 512  
182 kHz, 128 ms sampling time, and a frequency resolution of 7.81 Hz were generated for each point.

#### 183 **2.5 Data Analysis**

184 Experimental data was either analysed directly with the PSV software or with custom written scripts  
185 in Matlab (R2019a; The MathWorks Inc., Natick, MA, USA). Instantaneous phase in the time domain  
186 was obtained with Hilbert transform using custom Matlab code (Hartmann, 1997). We tested whether  
187 the frequency differed between left and right wings, and between areas (mirror, harp, chord, anal 1,  
188 anal 2) using linear mixed effects models run in R 4.0.0 (R Core Team, 2020). Models were run  
189 separately for free and engaged wings, with male ID included as a random effect. Models were run  
190 using lme4 (Bates et al., 2015) and lmerTest (Kuznetsova et al., 2017), with *post hoc* testing carried  
191 out using emmeans (Lenth, 2020). We also test the difference in the normalised amplitude of the  
192 mechanical response ( $\mu\text{m}/\text{Pa}$ ), between left and right wings using a paired t test.

193

### 194 **3 Results**

195 Using focal microinjection of the neuroactivator eserine into the cricket's brain (Wenzel et al., 1998;  
196 Hedwig, 2000), long-lasting and stable stridulation was elicited in 14 restrained males (Supplementary  
197 Video S1). Using two synchronized micro-scanning LDVs, we successfully measured the spatially  
198 resolved vibration of both wings simultaneously during the 'engaged' phase of the stridulation process  
199 in 11 of the 14 actively singing males, following a previously established protocol (Montealegre-Z et  
200 al., 2011). After the cessation of singing, the wings of each specimen were extended and fixed basally  
201 and stimulated with sweeps of broadband sound to reveal their natural resonances  $f_0$  and relative  
202 magnitudes of vibration. The surface area of these 'unengaged' wings was scanned in its  
203 entirety, providing a detailed map of vibrational patterns (Figs. 2 & 3 and Supplementary Video 2,  
204 showing wing vibrations of one male at resonance of 4.6 kHz).

### 205 3.1 Natural frequencies of wing vibrations

206 Full wing scan recordings of unengaged (extended and fixed) wings show that the RW  $f_0$  is  
 207 significantly higher than the LW (RW=5.168  $\pm$  0.434 kHz, SE 0.116; LW=4.827  $\pm$  0.396 kHz, SE  
 208 0.106; LMM:  $F_{1,152.60} = 15.93$ ,  $p < 0.001$ ). However, when comparing vibration amplitudes at the  
 209 average  $f_0$  of both wings, no difference between left and right wings was found. This was true for  
 210 both average vibration amplitudes per wing and maximum vibration amplitudes of the harp areas  
 211 alone (RW<sub>harp</sub>=0.32  $\pm$  0.24  $\mu\text{m}/\text{Pa}$ ; LW<sub>harp</sub>=0.40  $\pm$  0.35  $\mu\text{m}/\text{Pa}$ ;  $t=0.988$ ,  $df=13$ ,  $p=0.34$ ). When  
 212 each wing is stimulated at its average  $f_0$ , one always exhibits a higher vibration amplitude (on  
 213 average by a factor of  $\sim 1.7$ ; Fig. 2b, c), but this dominant wing can be either LW or RW (cf.  
 214 Supplementary Video 2, where the animal's left wing vibrates with higher amplitude). In a previous  
 215 study, we reported a trend of LW dominance which we could not identify here, which is most  
 216 likely due to our low sample size ( $n=44$  in Montealegre-Z et al., 2011).

217 Examining wing vibrations in more detail, LDV measurements reveal that each wing region exhibits  
 218 its own resonance spectra with varying peak frequencies (Fig. 3A); there were significant differences  
 219 in the  $f_0$  between areas (LMM:  $F_{4,152.56} = 72.55$ ,  $p < 0.001$ ). Post hoc testing revealed that the mirror of  
 220 each wing consistently showed higher  $f_0$  than the average wing  $f_0$  (LW<sub>mirror</sub>= 6.858  $\pm$  0.540 kHz, SE  
 221 0.127 kHz; LW average  $f_0$  of other areas = 4.827  $\pm$  0.396 kHz, SE 0.106; RW<sub>mirror</sub>= 7.007  $\pm$  0.865  
 222 kHz, SE 0.204 kHz; RW average  $f_0$  of other areas = 5.168  $\pm$  0.434 kHz, SE 0.116;  $n=18$ ) (Fig. 3A),  
 223 with other areas of the wing not significantly different from each other.

### 224 3.2 Wing vibrations in stridulating animals

225 Wing vibrations were recorded during active stridulation using two LDVs in single shot mode,  
 226 enabling vibration measurement at defined locations and times (see Supplementary Video 2).  
 227 Remarkably, vibrations of engaged wings during stridulation (Fig. 3B) differ from sound-evoked  
 228 vibrations in unengaged wings (Fig. 3A). When the wings are engaged, all regions exhibit near  
 229 identical, narrow vibrational frequency spectra with maximum power concentrated at the carrier  
 230 frequency  $f_c$  of the calling song (here 5.125 kHz; LMM:  $F_{3,66.29} = 1.56$ ,  $p=0.208$ ; Fig. 3B). There  
 231 is also no difference between the left or right wing (LMM:  $F_{1,65.20} = 0.77$ ,  $p=0.383$ ). The  
 232 convergence of all resonators towards one very narrow frequency band of oscillation is reminiscent  
 233 of entrainment, a process similar to synchronization between Huygens' clocks (Peña Ramirez et al.,  
 2016).

234  
 235 Apart from identical oscillation frequency, an additional key feature of synchronized resonators is  
 236 their phase relationship. Time-resolved LDV data were obtained by recording vibrations from  
 237 different regions of both wings at synchronised points during stridulation (see methods). Results  
 238 across 11 specimens show that the wings are not perfectly in phase during sound production, but that  
 239 phase lags  $\phi$  exist over a wide range between left and right wings (Fig. 4). In some individuals,  $\phi$   
 240 is small and relatively constant between wings (both over time and between regions, Fig. 4A), while  
 241 others show larger differences in phase (Fig. 4B and Fig. S1). Within an individual, average phase  
 242 lags across wing regions seem to be relatively consistent, although considerable variation exists (see  
 243 Fig. S1).

244 Time domain recordings of single point measurements at the harps, anal regions and mirrors also  
 245 show that LW vibration amplitudes are mostly higher than RW amplitudes (red and blue lines in  
 246 Fig. 4A, respectively) but there is also considerable variation in amplitudes across animals and  
 247 wing regions (Fig. 4B). The high variation in vibration amplitude can be explained by the  
 248 limitations of the experimental set up. As two lasers had to be manually aligned on the  
 stridulating animals, space restrictions and changes in the way the animals held their wings during  
 stridulation often prevented a perfect orthogonal alignment of the laser beams to the vibrating  
 surfaces, resulting in absolute

249 displacement amplitudes that are hard to compare between wings. Relative phase relationships  
 250 between the wings, however, can be measured with high accuracy, as they are not affected by laser  
 251 beam–target orthogonality. In theory, mathematical superposition of LW and RW vibrations allows  
 252 estimating the resulting combined output vibration. For example, the net vibratory response at a  
 253 given place and time caused by the two harps is the sum of the responses which would have been  
 254 caused by each harp individually (Fig. 5AB). These calculations show that the greater the phase lag  
 255  $\phi$  (and thus time lag  $\Delta t$  for a given frequency; cf. Figs. S1 & S2) between LW and RW, the lower  
 256 the amplitude of the resulting vibration and therefore the gain as compared to using only one  
 257 wing (Fig. 5AB and C). Without exact amplitude information for engaged wings, we can  
 258 nevertheless show the effect of phase shifts between wings on the overall output amplitude assuming  
 259 that vibration amplitudes are equal for both wings (as shown in Fig. 5A). Thus, Fig. 5C shows  
 260 normalised RMS (root mean square) gain as a function of phase lag  $\phi$  of three different wing regions  
 261 using normalised vibration velocity amplitudes. In ideal conditions, where both wings exhibit equal  
 262 vibration amplitudes at equal frequencies, perfect phase locking ( $\phi=0^\circ$ ) produces a gain of 2, while  
 263 a phase lag of  $120^\circ$  ( $\Delta t=67 \mu\text{s}$  at 5 kHz) would produce a gain of 1 or no amplification of the  
 264 resulting output as compared to using only one resonating wing. For example, the phase lags  
 265 recorded from left and right harps (median values ranging from  $6^\circ$  to  $79^\circ$  across all specimens; this  
 266 equates to  $\Delta t$  values between 3–43  $\mu\text{s}$ ; see Fig. S1, S2) produce relative amplitude gains ranging from  
 267 1.97 to 1.34 (Fig. 5C, blue stars). Other wing regions (mirror and anal regions, red circles and yellow  
 268 squares, respectively), exhibit similar values.

269 Fig. 5D illustrates the effect imperfect coupling of the wings has on the overall combined  
 270 output amplitudes at different song carrier frequencies (assuming both wings vibrate with the same  
 271 frequency and amplitude). While animals producing pure-tones at 5 kHz can afford to have relatively  
 272 uncoupled wings with time lags up to  $\sim 67 \mu\text{s}$  before destructive interference occurs (Fig. 5D,  
 273 intersection of blue and grey dashed lines),  $\Delta t$  at which destructive interference starts is reduced to  
 274  $\sim 48 \mu\text{s}$  and  $34 \mu\text{s}$  when singing at 7 or 10 kHz, respectively (red and yellow lines). The inset in Fig.  
 275 5D showing the average time differences and standard deviations between wings for the 11  
 276 specimens recorded shows that the span of  $\Delta t$  values (like  $\phi$ ) is generally small enough to ensure  
 277 amplitude gains well over 1.5 when singing with a 5 kHz carrier frequency.

## 278 4 Discussion

279 Here, we have revealed the presence of an elegant additional mechanism at work in crickets that  
 280 contributes to generating high amplitude, pure tone signals using distinct yet coupled sound generators:  
 281 the two forewings and their cellular structures. Although the wings appear to be mirror images of each  
 282 other (Fig. 1), they are asymmetrical in their mechanical properties and structure (Fig. 2A), as  
 283 previously reported (Simmons and Ritchie, 1996; Bennet-Clark, 2003; Montealegre-Z et al., 2011).  
 284 For *G. bimaculatus*, it is known that the RW on top is slightly larger in surface area and exhibits a  
 285 higher  $f_0$  than the LW (Montealegre-Z et al., 2011).

286 In addition, differences in resonant properties between both wings and among single wing regions are  
 287 characterised in some detail. The biomechanical data demonstrate that, within a single wing, different  
 288 regions have variable resonance peaks close to that of the harp  $f_0$  value and overall resonance curves  
 289 also differ in their spectral composition (Fig. 3). Interestingly, the observed differences between both  
 290 the individual wing regions and between the wings themselves (Fig. 3A), vanish when the wings  
 291 engage in active stridulation (Fig. 3B). These results confirm for the first time that all regions of both  
 292 wings actively radiate sound at the carrier frequency during stridulation and that the resonance

293 properties of the LW dominate the frequency output. This suggests that, during stridulation, the LW  
 294 harp vibrations, generated through plectrum-teeth impacts, drive the vibrations of all other  
 295 wing regions, including those of the RW, so that the engaged wings vibrate together at the LW  $f_0$ .

296 In order to produce the best possible signal output from both coupled resonators, we hypothesised  
 297 that both wings and the wing regions therein should not only oscillate at one common frequency, but  
 298 also, ideally, in-phase ( $\varphi=0^\circ$ ), thereby creating maximal constructive interference (and thus a  
 299 two-fold amplitude gain as compared to using only one wing). Whilst the whole system is indeed  
 300 driven and oscillating at one specific frequency, we find considerable incoherence in the phase  
 301 relationships between LW and RW and their respective regions. Figures 4 and 5 clearly show that  
 302 individual wing regions are not phase-locked to each other but exhibit average phase differences  $\varphi$   
 303 ranging from ca.  $6^\circ$  to  $79^\circ$ , equating to temporal differences  $\Delta t$  between the wings of 3-43  $\mu\text{s}$  at  
 304 the carrier frequency ( $f_c=5.125$  kHz). Figs. 4 and S1 also show that individuals exhibit roughly  
 305 similar phase differences within their wing regions but phase shifts between individuals are quite  
 306 variable. This leads us to suggest that the ability to tightly control the wing movements and the  
 307 coupling of the resonators is an individual trait depending on either wing morphology or neuro-  
 308 muscular control of the stridulation process or a combination thereof. As a consequence, the phase  
 309 differences  $\varphi$  and corresponding time lags  $\Delta t$  seen across the recorded individuals would approach  
 310 the distribution of this trait over the population.

311 Fig. 5AB depicts the consequences of these phase shifts in two male crickets on the opposite sides of  
 312 the range of observed  $\varphi$ . While the lower  $\varphi$  of Male 1 ( $\varphi=5.3^\circ$ ,  $\Delta t=2.9$   $\mu\text{s}$ , Fig. 5A) results in a  
 313 considerable output gain in comparison to the individual harp amplitudes (ca. 1.85 times the highest  
 314 LW amplitude), the higher phase differences of Male 2 ( $\varphi=58^\circ$ ,  $\Delta t=28$   $\mu\text{s}$ , Fig. 5B) result in only  
 315 a moderate gain (ca. 1.3). For this animal, a further increase in  $\varphi$  and consequently  $\Delta t$  would result  
 316 in destructive interference, whereby the combined output of both wings would be less than the output  
 317 of one wing alone, negating the advantage of using coupled resonators. This is shown in more detail  
 318 for three major wing regions over all animals in Fig. 5C. It is noteworthy that no instance of  
 319 destructive interference was observed in the specimens studied.

320 Fig. 5D shows the effects frequency has on the overall gain of this imperfect coupling in the temporal  
 321 domain. While a cricket singing at 5 kHz will experience an increase in combined output amplitude  
 322 (gain>1, above dashed grey line, Fig. 5D) for temporal differences between the wings of up to 67  $\mu\text{s}$   
 323 (corresponding to a  $120^\circ$  phase shift and assuming equal vibration amplitudes), crickets singing  
 324 at higher frequencies will encounter this threshold much earlier (at 48  $\mu\text{s}$  and 33  $\mu\text{s}$  for 7 kHz and 10  
 325 kHz, respectively). Consequently, the animals' observed inability to tightly synchronise the  
 326 wing movements in time will act as an acoustic constraint for crickets to exploit higher song  
 327 frequencies using two (imperfectly) coupled resonators. In addition, Fig. 5CD demonstrate that  
 328 the observed imperfections in wing coupling in *G. bimaculatus* are still sufficiently low to  
 329 ensure theoretical amplitude gains well above 1.5 times in comparison to the output of one wing  
 330 alone. It is unknown, however, if  $\varphi$  and  $\Delta t$  are, for example, dependent on temperature. Due to the  
 331 clockwork escapement mechanism involved in stridulation (and different from wing motion  
 332 dynamics; Prestwich and Walker, 1981) tooth strike rates and  $f_c$  are largely independent of  
 333 temperature in many Gryllidae, as are the resonant properties of the wings (Elliott and Koch, 1985;  
 334 Bennet-Clark and Bailey, 2002). However, some species can show slight changes in  $f_c$  with  
 335 temperature. Furthermore, the temporal song patterns, including syllable duration, are often affected  
 336 by changes in ambient temperature (Pires and Hoy, 1992; Walker and Cade, 2003). It would  
 337 therefore be conceivable that  $\varphi$  is also temperature dependent, potentially increasing with  
 temperature and changes in singing behaviour. Further experiments



338 including other cricket species and varying recording temperatures are planned to address inter-species  
339 variability and temperature dependence of the animals' wing coupling abilities.

340 If the higher values of  $\Delta t$  we observe in *G. bimaculatus* (Fig. 5D for averages and std; see Fig. S2 for  
341 a depiction of the range of observed values across all animals) are an indicator for the minimal  
342 amount of temporal control crickets in general are able to exert during stridulation, then one can  
343 attempt to calculate a cut-off frequency above which the sound production with two symmetrical  
344 and coupled wings becomes inefficient. The highest median value for  $\phi$  we measured for the three  
345 wing regions were between  $72^\circ$  and  $80^\circ$ , equating to  $\Delta t$  values between 38-43  $\mu\text{s}$  at  $f_c=5.125$  kHz.  
346 Using simple trigonometric relationships between phase, amplitude,  $\Delta t$  and frequency of waves  
347 and under the simplified assumption that both waves have the same frequency and amplitude, one  
348 can calculate the frequency  $f_{max}$  at which the gain of the combined output of the superimposed waves  
becomes 1:

$$349 \quad f_{max} = \arccos\left(\frac{Gain}{2}\right) / (\pi * \Delta t) \quad (1)$$

350 Using (1) and the range of  $\Delta t$  stated above, theoretical  $f_{max}$  values range from 7.8 kHz to 8.8 kHz (for  
351 43  $\mu\text{s}$  and 38  $\mu\text{s}$ , respectively), denoting frequencies above which stridulation using the  
352 mechanism described above becomes inefficient for some animals in the population. Taking the  
353 mean and standard deviation values for  $\Delta t$  shown in Fig. 5D as rough population measure (harp:  
354  $19.3 \pm 14.1$   $\mu\text{s}$ ; mirror:  $23.9 \pm 10.8$   $\mu\text{s}$ ; anal region:  $18.7 \pm 12.5$   $\mu\text{s}$ ; see also Fig. S2 & S3), one could  
355 state that ~16% of males would not be able to produce song above ~10 kHz with an amplitude gain  
356 above 1 when using both wings as active resonators.

357 These cut-off frequencies correspond very well with maximal carrier frequencies observed in the  
358 majority of Gryllidae, which lie between 2-8 kHz (Bennet-Clark, 1989; Robillard et al., 2015). A  
359 notable exception are members of the subfamily Eneopterinae, which produce calling songs  
360 with frequencies of up to 26 kHz (Robillard et al., 2013). Interestingly, in this subfamily, there is a  
361 clear gap between species singing at low frequencies and species singing at high frequencies. This  
362 gap is located between 7.9 and 12.2 kHz and members of the high-singing species form a distinct  
363 clade within the Eneopterinae (the Lebinthini) (Desutter-Grandcolas and Robillard, 2004).  
364 Additionally, Robillard *et al.* found that these species exhibit resonance patterns and stridulation  
365 mechanisms quite different to the ones employed by other Gryllids and other Eneopterinae  
366 (Robillard et al., 2013). Here, the resonances in the LW and RW are clearly asymmetrical, only  
367 partly (or not at all) overlapping the carrier frequencies and they generally show lower vibration  
368 magnitudes when compared to e.g. the wings of *G. bimaculatus*. Furthermore, instead of  
369 employing constant tooth strike rates (like *G. bimaculatus* and most other gryllids), some  
370 Lebinthini employ a stridulation mechanism (resembling those commonly observed in bush-crickets)  
371 whereby the wing stops during the closing phase to build up elastic energy which is then quickly  
372 released to produce highly increased tooth strike rates and therefore higher frequency calls  
373 (Robillard et al., 2013). These adaptations for high-frequency song production are similar to those  
374 encountered in bush-crickets. In bush-crickets, the wings are generally highly asymmetric as well,  
375 both morphologically and acoustically: The LW (lying on top of the RW and bearing the active  
376 stridulatory file) is often thicker, usually shows no clear stridulatory fields and is highly damped,  
377 therefore playing only a minor role in sound radiation (Montealegre-Z and Postles, 2010; Baker et  
378 al., 2017). The RW on the other side (which receives its mechanical input via the plectrum)  
379 often exhibits extremely thin to translucent stridulatory fields with clear resonance  
380 properties, thus constituting the acoustically active wing (e.g. Sarria-S et al., 2014; Baker et al.,  
381 2017). Thus, the sound production system in Tettigoniidae only contains one resonator, reducing the  
382 surface for sound radiation, whilst eliminating the problems inherent to two imperfectly coupled  
resonators as described here for crickets. This allows for a shift to higher song frequencies (and  
shorter wavelengths)

383 without destructive interference from a second resonator, and simultaneously ensures that the size of  
384 the remaining resonator is still (closer to) optimal for pure tone sound radiation.

385 In conclusion, the results presented here suggest a mechano-acoustical constraint on the bilateral near-  
386 symmetrical, dual resonator sound production mechanism common to most Gryllidae which prevents  
387 the exploitation of higher song frequencies above ~8-9 kHz whilst still being able to produce loud and  
388 pure-tone calling songs to effectively attract mates. This could have been an important constraint for  
389 the majority of Gryllidae (restricting them to the role of tenors) which the Tettigoniidae (the sopranos  
390 within the Ensifera) seem to have overcome by evolving a highly asymmetric singing mechanism  
391 (Montealegre-Z et al., 2017; Song et al., 2020) which allows them to produce high-frequency songs  
392 without the drawback of undesirable destructive interference reducing song amplitude.

393

## 394 **5 Author contributions**

395 F.M.-Z., T.J., and D.R. designed research; F.M.-Z., and T.J. performed experiments; CS conducted  
396 statistics; F.M.-Z., T.J. and CS analysed data; and F.M.-Z., T.J. and D.R. wrote the paper. F.M.-Z. and  
397 T. J. contributed equally to this work.

398

## 399 **6 Conflict of interest**

400 The authors declare no conflict of interest.

401

## 402 **7 Funding**

403 This research was supported by a Leverhulme Trust grant (grant RPG-2014-284 to F.M.-Z. & D.R.), a  
404 Human Frontier Science Programme (Cross Disciplinary Fellowship LT00024/2008-C to F.M.-Z.) and  
405 a National Geographic grant (National Geographic Explorer's grant RG120495 to F.M.-Z.). D.R. also  
406 acknowledges the support of the Royal Society of London, by the UK–India Education and Research  
407 Initiative (grant no. SA06-169E to D.R.) and the Biotechnology and Biological Sciences Research  
408 Council. T.J. was supported through a Human Frontier Science Programme grant during the  
409 experimental phase and by the European Commission via a Horizon 2020 Marie Skłodowska-Curie  
410 fellowship (No. 829208, InWingSpeak).

411

## 412 **8 Acknowledgments**

413 We thank the editor and three reviewers for their helpful comments on the manuscript.

414

## 415 **9 References**

- 416 Baker, A., Sarria-S, F. A., Morris, G. K., Jonsson, T., and Montealegre-Z, F. (2017). Wing Resonances  
 417 in a New Dead-Leaf-Mimic Katydid (Tettigoniidae: Pterochrozinae) From the Andean Cloud  
 418 Forests. *Zool. Anz.* 270, 60–70. doi: 10.1016/j.jcz.2017.10.001
- 419 Bates, D., Mächler, M., Bolker, B., and Walker, S. (2015). Fitting Linear Mixed-Effects Models Using  
 420 Lme4. *J. Stat. Soft.* 67. doi: 10.18637/jss.v067.i01
- 421 Bennet-Clark, H. C. (1989). “Songs and the Physics of Sound Production,” in *Cricket Behavior and*  
 422 *Neurobiology*, eds. F. Huber, T. E. Moore, and W. Loher (Ithaca, N.Y. Comstock Publishing  
 423 Associates), 227–261.
- 424 Bennet-Clark, H. C. (1998). Size and Scale Effects as Constraints in Insect Sound Communication.  
 425 *Philos. Trans. R. Soc. London, Ser. B* 353, 407–419. doi: 10.1098/rstb.1998.0219
- 426 Bennet-Clark, H. C. (1999). Resonators in Insect Sound Production: How Insects Produce Loud Pure-  
 427 Tone Songs. *J. Exp. Biol.* 202, 3347–3357.
- 428 Bennet-Clark, H. C. (2003). Wing Resonances in the Australian Field Cricket *Teleogryllus oceanicus*.  
 429 *J. Exp. Biol.* 206, 1479–1496. doi: 10.1242/jeb.00281
- 430 Bennet-Clark, H. C., and Bailey, W. J. (2002). Ticking of the Clockwork Cricket: The Role of the  
 431 Escapement Mechanism. *J. Exp. Biol.* 205, 613–625.
- 432 Desutter-Grandcolas, L., and Robillard, T. (2004). Acoustic Evolution in Crickets: Need for  
 433 Phylogenetic Study and a Reappraisal of Signal Effectiveness. *Anais da Academia Brasileira de*  
 434 *Ciências* 76, 301–315.
- 435 Elliott, C. J. H., and Koch, U. T. (1985). The Clockwork Cricket. *Naturwissenschaften* 72, 150–153.  
 436 doi: 10.1007/BF00490404
- 437 Fletcher, N. H. (1992). *Acoustic Systems in Biology*. Oxford: Oxford University Press.
- 438 Forrest, T. G., and Green, D. M. (1991). Sexual Selection and Female Choice in Mole Crickets  
 439 (*Scapteriscus*: Gryllotalpidae): Modelling the Effects of Intensity and Male Spacing. *Bioacoustics*  
 440 3, 93–109. doi: 10.1080/09524622.1991.9753166
- 441 Gu, J.-J., Montealegre-Z, F., Robert, D., Engel, M. S., Qiao, G.-X., and Ren, D. (2012). Wing  
 442 Stridulation in a Jurassic Katydid (Insecta, Orthoptera) Produced Low-Pitched Musical Calls to  
 443 Attract Females. *PNAS* 109, 3868–3873. doi: 10.1073/pnas.1118372109
- 444 Hartmann, W. M. (1997). *Signals, Sound, and Sensation*. Woodbury, N.Y: American Institute of  
 445 Physics.
- 446 Hedwig, B. (2000). Control of Cricket Stridulation by a Command Neuron: Efficacy Depends on the  
 447 Behavioral State. *J. Neurophysiol.* 83, 712–722.
- 448 Hedwig, B., and Becher, G. (1998). Forewing Movements and Intracellular Motoneurone Stimulation  
 449 in Tethered Flying Locusts. *J. Exp. Biol.* 201, 731.
- 450 Koch, U. T., Elliott, C. J. H., Schöffner, K.-H., and Kleindienst, H.-U. (1988). The Mechanics of  
 451 Stridulation of the Cricket *Gryllus campestris*. *J. Comp. Physiol.* 162, 213–223. doi:  
 452 10.1007/BF00606086
- 453 Kostarakos, K., Hartbauer, M., and Römer, H. (2008). Matched Filters, Mate Choice and the Evolution  
 454 of Sexually Selected Traits. *Plos One* 3, e3005. doi: 10.1371/journal.pone.0003005
- 455 Kuznetsova, A., Brockhoff, P. B., and Christensen, R. H. B. (2017). lmerTest Package: Tests in Linear  
 456 Mixed Effects Models. *J. Stat. Soft.* 82. doi: 10.18637/jss.v082.i13

- 457 Lenth, R. (2020). *emmeans: Estimated Marginal Means, Aka Least-Squares Means*.
- 458 Michelsen, A. (1998). The Tuned Cricket. *News in Physiological Sciences* 13, 32–38.
- 459 Michelsen, A., and Larsen, O. N. (2008). Pressure Difference Receiving Ears. *Bioinspir. Biomim.* 3.
- 460 Montealegre-Z, F. (2005). *Biomechanics of Musical Stridulation in Katyids (Orthoptera: Ensifera:*  
461 *Tettigoniidae): An Evolutionary Approach*. Ph.D. Toronto: U. o. Toronto, Department of Zoology.
- 462 Montealegre-Z, F., Jonsson, T., and Robert, D. (2011). Sound Radiation and Wing Mechanics in  
463 Stridulating Field Crickets (Orthoptera: Gryllidae). *J. Exp. Biol.* 214, 2105–2117. doi:  
464 10.1242/jeb.056283
- 465 Montealegre-Z, F., and Postles, M. (2010). Resonant Sound Production in *Copiphora gorgonensis*  
466 (Tettigoniidae: Copiphorini), an Endemic Species from Parque Nacional Natural Gorgona,  
467 Colombia. *Journal of Orthoptera Research* 19, 347–355. doi: 10.1665/034.019.0223
- 468 Montealegre-Z, F., Ogden, J., Jonsson, T., and Soulsbury, C. D. (2017). Morphological Determinants  
469 of Signal Carrier Frequency in Katyids (Orthoptera): A Comparative Analysis Using Biophysical  
470 Evidence of Wing Vibration. *J. Evol. Biol.* 30, 2068–2078. doi: 10.1111/jeb.13179
- 471 Nocke, H. (1971). Biophysik der Schallerzeugung durch die Vorderflügel der Grillen. *Z. vergl. Physiol.*  
472 74, 272–314. doi: 10.1007/bf00297730
- 473 Peña Ramirez, J., Olvera, L. A., Nijmeijer, H., and Alvarez, J. (2016). The Sympathy of Two Pendulum  
474 Clocks: Beyond Huygens' Observations. *Sci. Rep.* 6, 23580. doi: 10.1038/srep23580
- 475 Pires, A., and Hoy, R. R. (1992). Temperature Coupling in Cricket Acoustic Communication. I. Field  
476 and Laboratory Studies of Temperature Effects on Calling Song Production and Recognition in  
477 *Gryllus firmus*. *J. Comp. Physiol.* 171, 69–78. doi: 10.1007/bf00195962
- 478 Prestwich, K. N., Lenihan, K. M., and Martin, D. M. (2000). The Control of Carrier Frequency in  
479 Cricket Calls: A Refutation of the Subalar-Tegminal Resonance / Auditory Feedback Model. *J. Exp.*  
480 *Biol.* 203, 585–596.
- 481 Prestwich, K. N., and Walker, T. J. (1981). Energetics of Singing in Crickets: Effect of Temperature  
482 in Three Trilling Species (Orthoptera: Gryllidae). *J. Comp. Physiol.* 143, 199–212. doi:  
483 10.1007/BF00797699
- 484 R Core Team (2020). *R: A Language and Environment for Statistical Computing*. Vienna, Austria: R  
485 Foundation for Statistical Computing.
- 486 Robillard, T., Montealegre-Z, F., Desutter-Grandcolas, L., Grandcolas, P., and Robert, D. (2013).  
487 Mechanisms of High-Frequency Song Generation in Brachypterous Crickets and the Role of Ghost  
488 Frequencies. *J. Exp. Biol.* 216, 2001–2011. doi: 10.1242/jeb.083964
- 489 Robillard, T., ter Hofstede, H. M., Orivel, J., and Vicente, N. M. (2015). Bioacoustics of the  
490 Neotropical Eneopterinae (Orthoptera, Grylloidea, Gryllidae). *Bioacoustics* 24, 123–143. doi:  
491 10.1080/09524622.2014.996915
- 492 Römer, H. (1998). “The Sensory Ecology of Acoustic Communication in Insects,” in *Comparative*  
493 *Hearing: Insects*, eds. R. R. Hoy, A. N. Popper, and R. R. Fay (Springer New York), 63–96.
- 494 Rossing, T. D. (1990). *The Science of Sound*. Reading, Mass. Addison-Wesley.
- 495 Sarria-S, F. A., Buxton, K., Jonsson, T., and Montealegre-Z, F. (2016). Wing Mechanics, Vibrational  
496 and Acoustic Communication in a New Bush-Cricket Species of the Genus *Copiphora* (Orthoptera:  
497 Tettigoniidae) From Colombia. *Zool. Anz.* 263, 55–65. doi: 10.1016/j.jcz.2016.04.008

- 498 Sarria-S, F. A., Morris, G. K., Windmill, J. F. C., Jackson, J., and Montealegre-Z, F. (2014). Shrinking  
 499 Wings for Ultrasonic Pitch Production: Hyperintense Ultra-Short-Wavelength Calls in a New Genus  
 500 of Neotropical Katydid (Orthoptera: Tettigoniidae). *Plos One* 9. doi: 10.1371/journal.pone.0098708
- 501 Simmons, L. W., and Ritchie, M. G. (1996). Symmetry in the Songs of Crickets. *P. Roy. Soc. B-Biol.*  
 502 *Sci.* 263, 1305–1311. doi: 10.1098/rspb.1996.0191
- 503 Sismondo, E. (1993). Ultrasubharmonic Resonance and Nonlinear Dynamics in the Song of *Oecanthus*  
 504 *nigricornis* F. Walker (Orthoptera: Gryllidae). *Int. J. Insect Morphol. Embryol.* 22, 217–231. doi:  
 505 10.1016/0020-7322(93)90011-O
- 506 Song, H., Béthoux, O., Shin, S., Donath, A., Letsch, H., Liu, S., et al. (2020). Phylogenomic Analysis  
 507 Sheds Light on the Evolutionary Pathways Towards Acoustic Communication in Orthoptera. *Nat.*  
 508 *Commun.* 11, 4939. doi: 10.1038/s41467-020-18739-4
- 509 Walker, S. E., and Cade, W. H. (2003). The Effects of Temperature and Age on Calling Song in a Field  
 510 Cricket with a Complex Calling Song, *Teleogryllus oceanicus* (Orthoptera: Gryllidae). *Can. J. Zool.*  
 511 81, 1414–1420. doi: 10.1139/z03-106
- 512 Warren, P. S., Katti, M., Ermann, M., and Brazel, A. (2006). Urban Bioacoustics: It’s Not Just Noise.  
 513 *Anim. Behav.* 71, 491–502. doi: 10.1016/j.anbehav.2005.07.014
- 514 Wenzel, B., Elsner, N., and Hedwig, B. (1998). Microinjection of Neuroactive Substances into Brain  
 515 Neuropil Controls Stridulation in the Cricket *Gryllus bimaculatus* (De Geer). *Naturwissenschaften*  
 516 85, 452–454.
- 517 Wenzel, B., and Hedwig, B. (1999). Neurochemical Control of Cricket Stridulation Revealed by  
 518 Pharmacological Microinjections into the Brain. *J. Exp. Biol.* 202, 2203–2216.
- 519 Wiley, R. H. (2006). “Signal Detection and Animal Communication,” in *Advances in the Study of*  
 520 *Behavior*, eds. H. J. Brockmann, P. J. Slater, and C. T. Snowdon (London: Academic Press), 217–  
 521 247.

522

## 523 10 Figure captions

524 **Fig. 1:** Extended tegmina of *Gryllus bimaculatus*. (A) The main regions involved in sound production  
 525 are highlighted. Nomenclature of wing regions follows Montealegre-Z et al. (2011). (B) The problem  
 526 of phase interference during tegmino-tegminal stridulation. For the left, plectrum-bearing wing (PBW),  
 527 energy from tooth impacts will travel a constant distance (D) from the plectrum region to a specific  
 528 region of the same wing (e.g., the red dot; arbitrarily chosen). Conversely, for the file-bearing right  
 529 wing (FBW), the point of energy input will change as the scraper moves over the file. Energy will  
 530 travel different distances (D1, D2, D3), reaching the red dot at variable times t, resulting in varying  
 531 phases of vibration as the scraper moves.

532 **Fig. 2:** Amplitude response of extended wings to sympathetic acoustic stimulation. (A) Orientation  
 533 image relating tegmen topography to the position of the scanning lattice. (B) Scanned area and  
 534 deflection shapes of the tegmen dorsal surface (harp and mirror). Dashed lines illustrate the sections  
 535 through which the deflection envelopes in C were built. (C) Envelope of mechanical deflections along  
 536 transects shown in B for a series of phases (in steps of 10°) in the full oscillation cycle. For this  
 537 specimen: RW  $f_0=4.71$  kHz, LW  $f_0=4.62$  kHz).

538 **Fig. 3:** Wing region resonances of unengaged and engaged wings of a male *G. bimaculatus*. (A) Natural  
 539 resonances of wing regions measured with LDV in unengaged wings. (B) Wing resonances measured  
 540 in the same individual during stridulation (engaged). Vibration amplitudes have been normalized to a  
 541 relative dB scale.

542 **Fig. 4:** Vibration displacements and phase relation in three major wing regions during stridulation in  
 543 two *G. bimaculatus* males. Wing vibration measurements were obtained simultaneously from two  
 544 homologous wing regions using two LDVs. (A) An individual with nearly perfect phasing of the wings  
 545 (median  $\phi$  between  $6^\circ$  and  $15^\circ$ ). (B) An individual with more prominent phase differences and variation  
 546 between the wings (median  $\phi$  between  $60^\circ$  and  $68^\circ$ ). Each panel represents an independent recording  
 547 showing RW in blue, LW in red and phase lag  $\phi$  in grey.  $\phi$  is measured as the difference in phase  
 548 between LW and RW at the LW local maxima and minima. Boxplots show the median (red line), 25<sup>th</sup>,  
 549 75<sup>th</sup> percentiles (box) and 1 IQR whiskers for all  $\phi$  per wing region. Outliers are marked as red +.

550 **Fig. 5:** Sound wave superposition to illustrate amplitude gains. (A) Theoretical harp output calculated  
 551 from a *G. bimaculatus* showing small phase differences between both harps ( $\phi \sim 5^\circ$ ;  $\Delta t \sim 3 \mu\text{s}$ ;  $f_c = 5.07$   
 552 kHz). (B) Harp output from an individual with large phase differences ( $\phi \sim 58^\circ$ ;  $\Delta t \sim 28 \mu\text{s}$ ;  $f_c = 5.7$  kHz).  
 553 Note that in spite of large phase differences, the output (black outline) shows a gain, which is larger in  
 554 A. In both cases, tracks have been normalised to the highest amplitude. (C) Comparison of median  
 555 absolute phase lag per specimen and RMS gain of three major wing regions. Vibrations were obtained  
 556 simultaneously from the paired respective regions (harps, mirrors and anal) of LW and RW. RMS gains  
 557 were calculated from the superposition of normalised LW and RW displacement responses measured  
 558 with each laser. Each data point per region represents one individual;  $n=11$ . The solid line shows  
 559 theoretical gains with increasing  $\phi$  assuming equal **vibration** amplitudes and frequencies. (D) Mean  
 560 absolute time lags  $\Delta t$  (black circles) and standard deviation between LW and RW for three major wing  
 561 regions and 11 animals. Coloured solid lines show the theoretical amplitude gains (right y-axis in grey;  
 562 equal amplitudes and frequencies) as function of  $\Delta t$  for three different carrier frequencies (blue, red  
 563 and yellow for 5, 7 and 10 kHz, respectively). Values below 1 (dashed grey line) signify lower  
 564 combined output amplitudes compared to using only one resonator.

565

## 566 11 Video captions

567 **Video 1:** A male *Gryllus bimaculatus* producing calling song in the experimental setup after  
 568 pharmacological injection of Eserine ( $10^{-2}$  mol/l) into the brain. The cricket is mounted and fixed on  
 569 a holder in front of the LDV. The LDV's laser dot is visible on the harp area of the right wing.

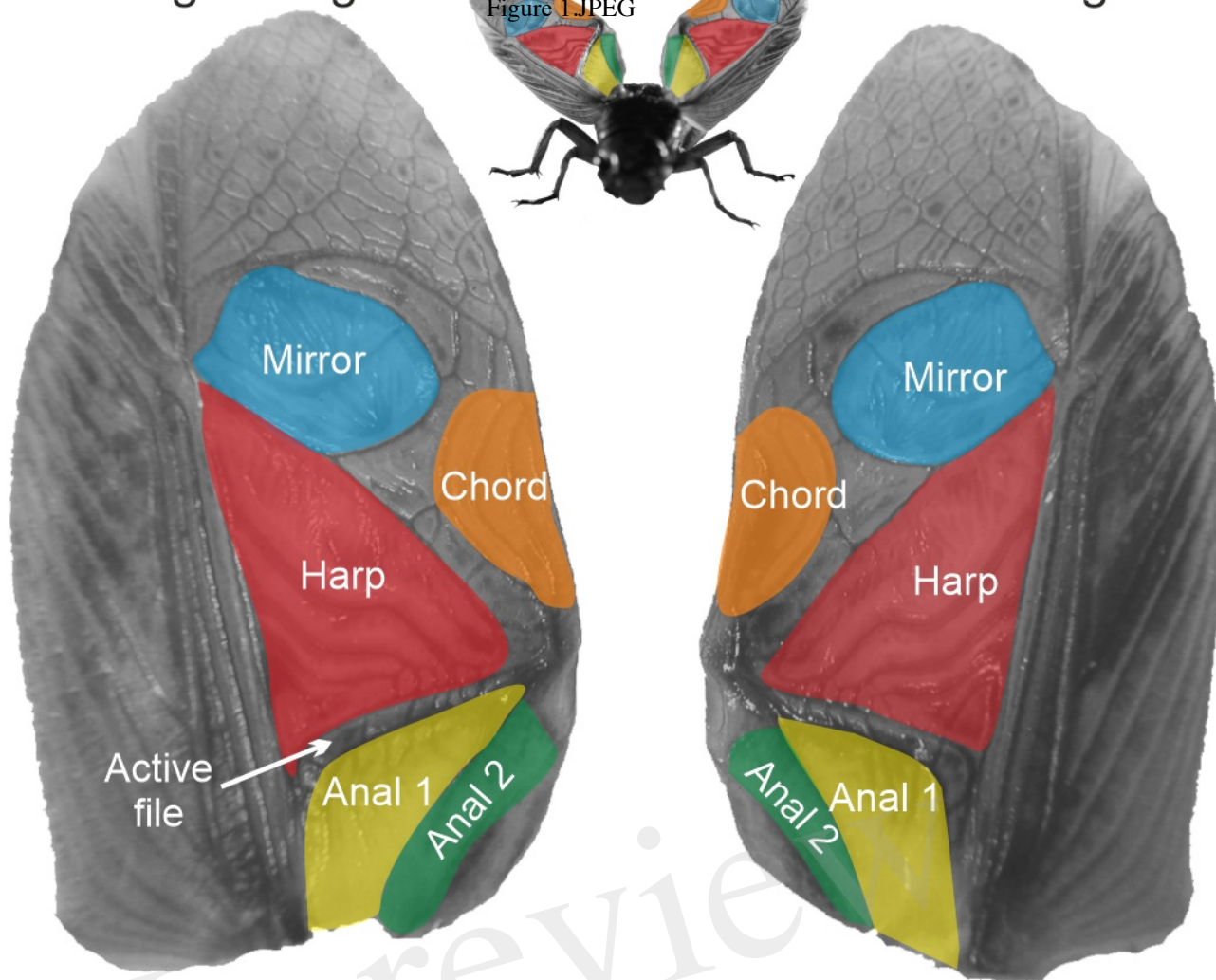
570 **Video 2:** Animation of the vibration map of unengaged left and right wing of a male  
 571 *Gryllus bimaculatus* as derived from LDV recordings. The wings are elevated upwards from the  
 572 animal's body at a similar angle to the natural singing position, spaced apart and imaged from the  
 573 front; the reference microphone is visible between and slightly behind the wings. The overlaid  
 574 vibration map shows the colour-coded relative displacement ( $\mu\text{m}/\text{Pa}$ ; red=max. positive  
 575 displacement; blue=max. negative displacement) of the wing surface as a response to acoustic  
 576 stimulation at the wings' overall resonance frequency (4.62 kHz). Here, the LW displacement  
 amplitude is higher than the RW's.

A

Right wing

Figure 1.JPEG

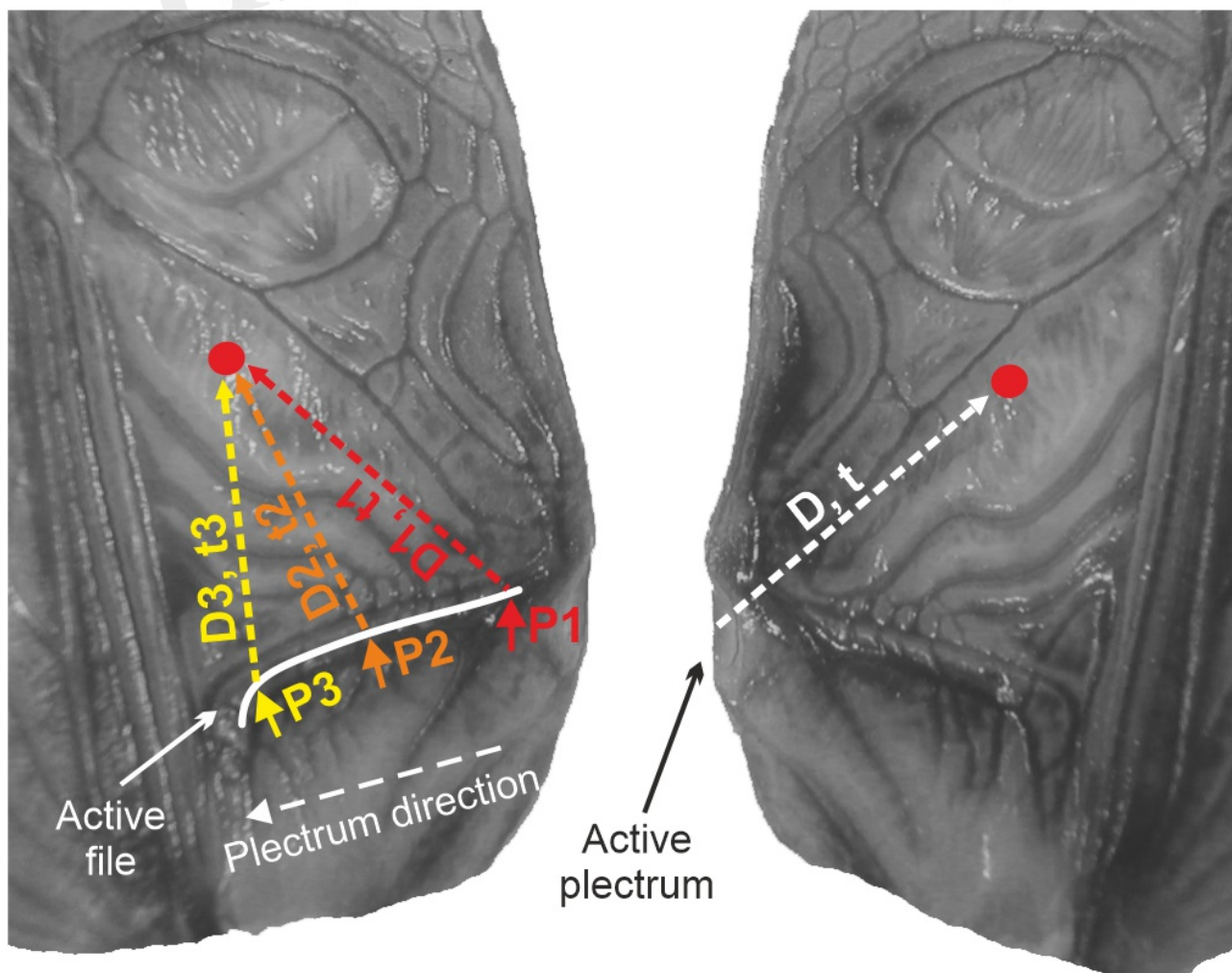
Left wing



B

RW (FBW)

LW (PBW)



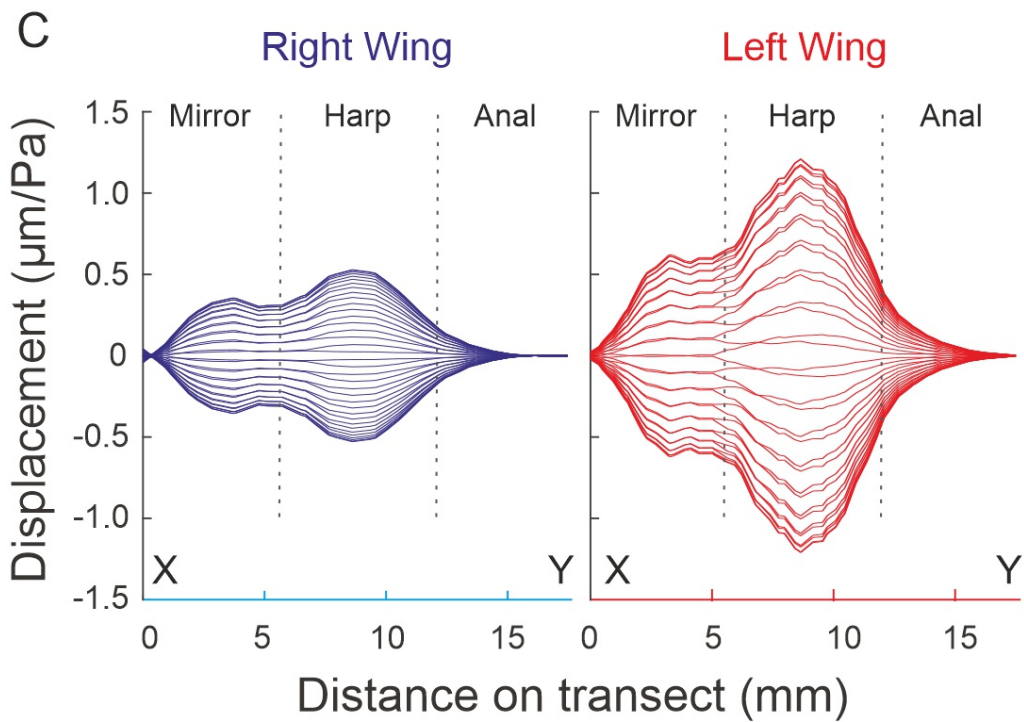
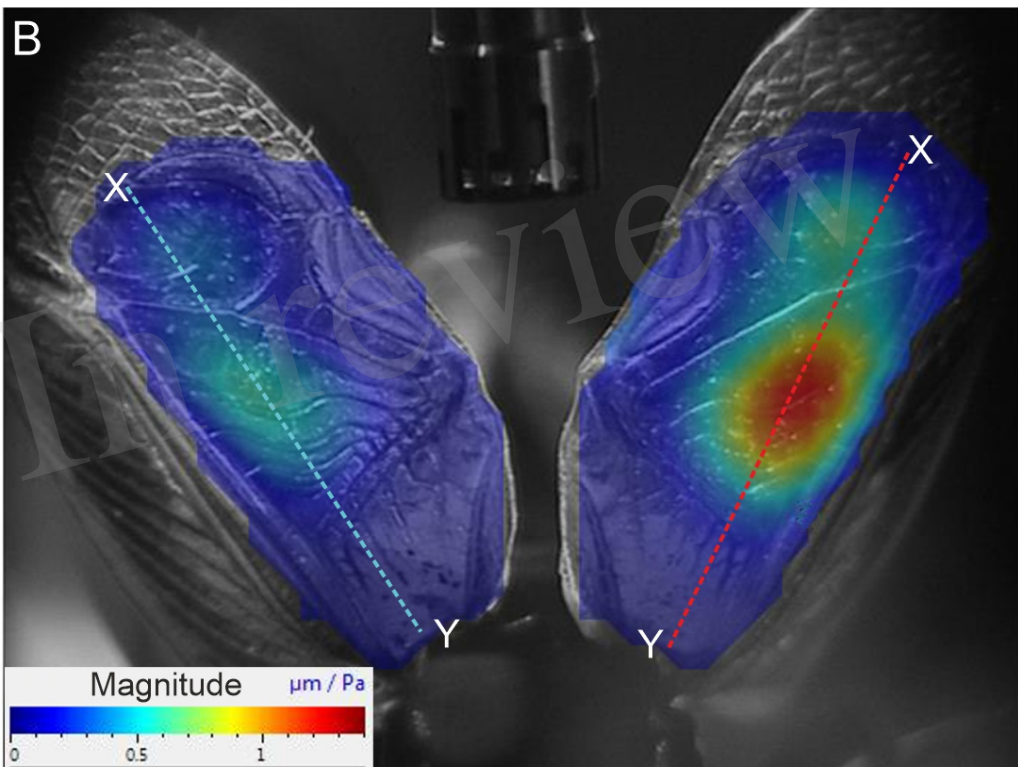
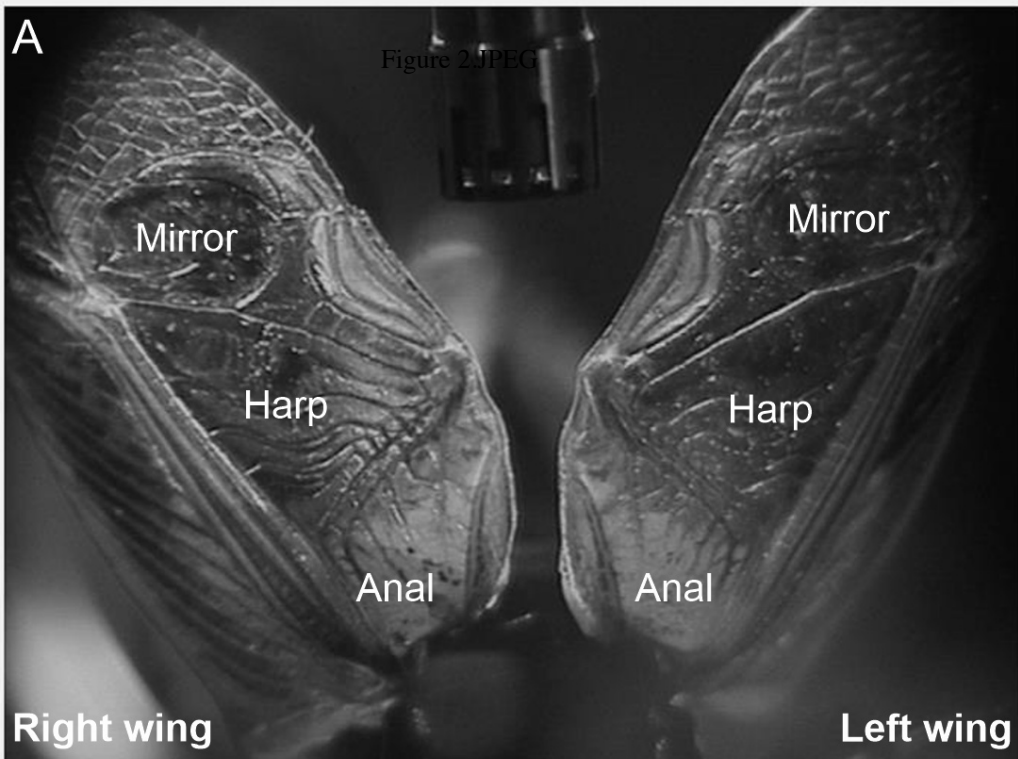
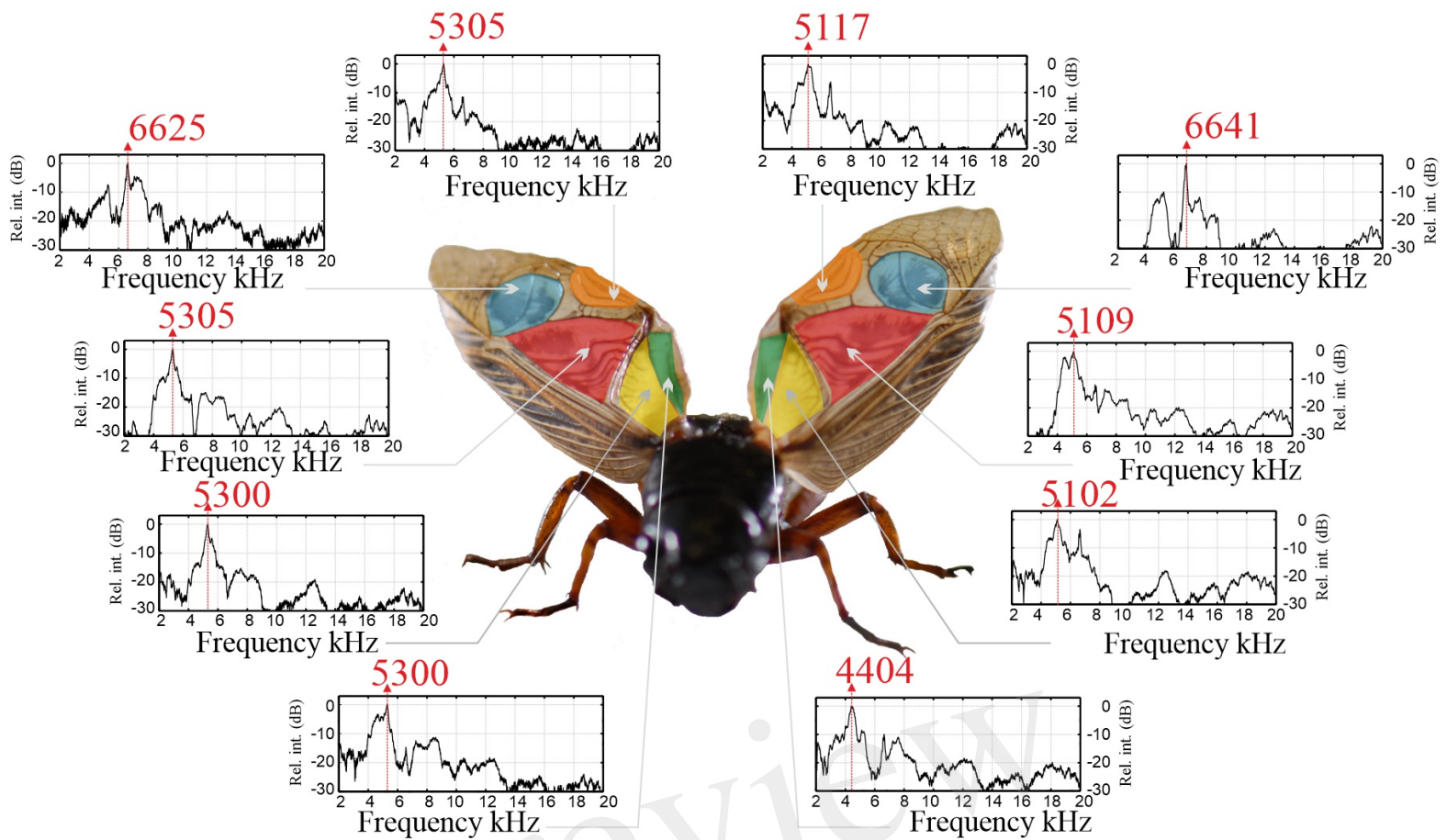




Figure 3.JPEG

### Free wing vibration



### B

### Wing vibration during stridulation

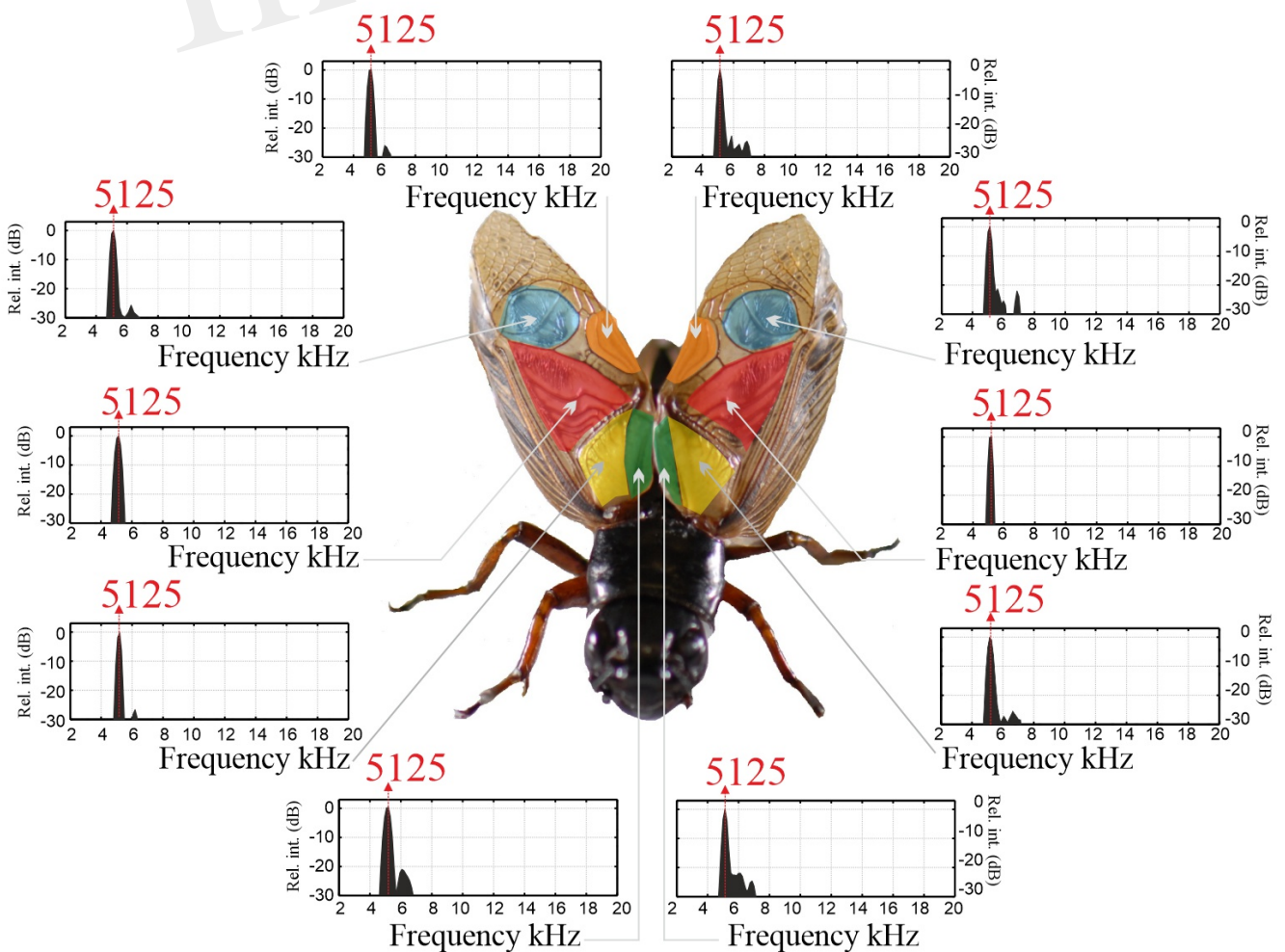


Figure 4.JPEG

